Available online at http://scik.org
Commun. Math. Biol. Neurosci. 2020, 2020:18
https://doi.org/10.28919/cmbn/4388
ISSN: 2052-2541

SYSTEM (GIS) AND THE MATHEMATICAL MODELING OF EPIDEMICS TO ESTIMATE AND CONTROL THE SPATIO-TEMPORAL SEVERITY OF INFECTION IN THE MOST ATTRACTIVE REGIONS

HAMZA BOUTAYEB[1], MUSTAPHA LHOUS[2], OMAR ZAKARY[1,*], MOSTAFA RACHIK[1]

[1]Laboratory of Analysis Modelling and Simulation, Department of Mathematics and Computer Science, Faculty of Sciences Ben M'Sik, Hassan II University of Casablanca, BP 7955, Sidi Othman, Casablanca, Morocco

[2]Laboratory of Modeling, Analysis, Control and Statistics, Department of Mathematics and Computer Science, Faculty of Sciences Ain Chock, Hassan II University of Casablanca, B.P 5366 Maarif Casablanca, Morocco

Abstract. To investigate the spatio-temporal spread of an epidemic in several regions (cities, towns, neighbors...) that are connected by population movements, we adopt a new generalized discrete-time multi-region SIR model, in which we introduce a new diffusion terms that describe the potential attractiveness of each region. In this work we study the effect of the potential attractiveness of regions, and we show the influence of one region on the others by varying attractiveness parameters associated to each zone. We determine an optimal control strategy which allows to reduce the infectious individuals and increase the number of recovered ones in a targeted region and this with an optimal cost. We investigate also the impact of these diffusion parameters on several control strategies by considering several control scenarios.

As an application of our theoretical results, first, we investigate the potential attractiveness of the Grand Casablanca-Settat region of Morocco. We calculated the potential attractiveness of each sub region of the studied area by using a qualitative method based on the use of topographic data as well as observations made in the field using the ArcGIS Geoprocessing Tool. The attractiveness map can help to simplify the implementation of control strategies, the organization of cultural events and the implementation of awareness campaigns.

*Corresponding author
E-mail address: zakaryma@gmail.com
Received November 24, 2019

Second, we use our new multi-region model to simulate the spread of an epidemic within these connected zones of the Grand Casablanca-Settat region. Examples and numerical simulations are given to illustrate the spread of infection and to illustrate the efficiency of the optimal control strategy. Results of that paper can be used by decision makers to identify and track the evolution of epidemics within a more complex system of connected zones.

Keywords: GIS; geoprocessing; attractiveness; mathematical modeling; multi-region; SIR model; optimal control.

2010 AMS Subject Classification: 39A05, 39A45, 39A60, 93C35, 93C55.

1. INTRODUCTION

Residents, businesses and visitors can be considered as the main groups in a society, and satisfaction of the needs of these three target groups in a region (city, town, ...) is the most important factor of its attractiveness. Several studies and research [1, 2] , define the attractive regions as the regions with the following potentialities: an enforced security, an effective structure of economic activities, successful business and housing policy, accessibility and mobility, access to public services and institutions, efficient transport and traffic system, knowledge-based society, information tools and resources, natural and physical environment; strong and diverse cultural and tourism sector, the city's vitality, liveability, viability and the city's image.

The attractiveness of regions allows these three groups of society to move from one region to another according to their needs. An attractive region for businesses should have a good accessibility, location, built environment, sufficient and quality workforce, quality of utilities, encouraging land prices, taxes and local requirements, new and existing customers, suppliers, finance, partners. For visitors, they are looking for temporary accommodation (hotels, apartments, campsites, family houses, etc.) of high quality at an acceptable cost, as well as accessibility to tourist sites, places of relaxation and entertainment (beaches, forests, theaters and playrooms), the availability of restaurants, parking, public transport, security, the cultural sector, and other amenities. However, an attractive city for residents should have a good, accessible, clean and secure environment, places for work (factories, large yards, important ports), institutions of education and health of quality, high-quality city culture, public safety, religious sites, green spaces, leisure facilities.

The importance of these features attracts individuals of all kinds whether it is a healthy or sick

person. This allows a sick person to move toward more attractive areas which lead to a rapid spread of infections and therefore an epidemic.

Mathematical modeling in epidemiology has become an important tool for analyzing the dynamics and spread of epidemics. Mathematical models provide a more in-depth insight into the spread of infectious diseases and enable authorities to make decisions to eradicate such epidemics.

Among the modeling methods of diseases is the use of the compartmental model, in which the population is divided into different groups according to the stage of the infection, with assumptions about the transfer rate of time from one compartment to the other. In the last decades, different epidemics have spread in a wide geographical area, such as HIV / AIDS: [3, 4, 5], Ebola [6, 7], Cholera [8, 9, 10], Malaria [11, 12] and Influenza [13, 14]. Thus the need for the incorporation of spatial spread of epidemics in mathematical models.

Based on all these ideas, in this paper, we propose a new mathematical modeling of epidemic by using a multi-region SIR model in which we incorporate the potential attractiveness of regions. To the best of the authors knowledge, this is the first work that use the potential attractiveness of regions in the spatial temporal spread of epidemics modeling.

We suggest a new discrete time model that describes the spread of an epidemic in a geographical area noted Ω, which is divided into sub-domains (cells) noted C_{pq}, where p and q denotes coordinates of that cell. All these cells are supposed to be connected by movements of their residents. The potential attractiveness of each cell is considered as a model parameter that will be mathematically defined later. We also investigate a control strategy which allows reducing the infectious individuals and increasing the number of recovered individuals and this with an optimal cost. To do this, we incorporate a control variable in the model describing the efficiency of vaccination campaigns and / or awareness programs that could be applied in the zone targeted by this control strategy. The optimal control problems are obtained based on a discrete version of Pontryagin's maximum principle, and resolved numerically using a progressive-regressive discrete scheme that converges following an appropriate test related to the Forward-Backward Sweep Method (FBSM) on optimal control. Numerical simulations are

performed to show the effectiveness of the optimal control strategy and to show the influence of the potential attractiveness of one region on the others.

In order to apply these results to show the influence of the potential attractiveness of regions on the spread of epidemics, we start by eliciting a geographic model to show how we can define potential attractive zones in the Grand Casablanca-Settat region, based on the use of map data using the powerful ArcGIS Geoprocessing tool. We collect data coordinates for four attractiveness factors: Hospitals, higher institutions, industrial zones and touristic places. We carry out the attractiveness map and then we use region attractiveness values in the multi-region SIR model to simulate the epidemic spread within the Grand Casablanca-Settat region by combining the ArcGIS and Matlab programs.

The paper is organized as follows: Section 2. presents the new discrete-time multi-region SIR epidemic model. Attractiveness parameters are mathematically defined. We present in the second subsection the optimal control problem. Simulations are carried out in the third subsection. In Section 3., we present a case study of the previous theoretical results by identifying the attractiveness map of the Grand Casablanca-Settat region, and then simulations of the numerical results are provided. Finally, we conclude the paper in Section 4.

2. Mathematical Model

2.1. Model description. We consider a multi-regions discrete-time epidemic model which describes SIR dynamics within a global domain of interest Ω which in turn is divided to M^2 regions or cells. In other words, $\Omega = \bigcup_{p,q=1,..,M} C_{pq}$ with C_{pq} denoting a spatial location or region. We note that $(C_{pq})_{p,q=1,...,M}$ could represent a country, a city or town, or a small domain, which belong respectively to the domain Ω which could represent a part of country or a whole country.

According to the disease transmission mechanism, the host population of each cell C_{pq} is grouped into three epidemiological compartments, $S_i(C_{pq})$ susceptible individuals, $I_i(C_{pq})$ infected individuals and $R_i(C_{pq})$ removed individuals of C_{pq} at time i.

We note that there are population movements among these three epidemiological compartments, from time unit i to time i + 1. We assume that the susceptible individuals of C_{pq} not yet infected but can be infected only through contacts with infectives of C_{pq} and $C_{rs} \in \mathscr{V}_{pq}$, where

$\mathscr{V}_{pq}$ is the vicinity set, composed by C_{pq} and all neighboring cells of C_{pq} which are denoted by $(C_{rs})_{r=p+k,s=q+k'}$ with $(k,k') \in \{-1,0,1\}^2$ except when $k = k' = 0$, thus

$$\mathscr{V}_{pq} = \left\{ C_{rs} \in \Omega / r = p+k, s = p+k', (k,k') \in \{-1,0,1\}^2 \right\}$$

and

$$\mathscr{V}'_{pq} = \mathscr{V}_{pq} \backslash C_{pq}$$

Therefore, the infection transmission is assumed to occur between individuals present in a given cell C_{pq}, and is given by $\sum_{C_{rs} \in \mathscr{V}_{pq}} \gamma(C_{rs}) S_i(C_{pq}) I_i(C_{rs})$, where $\gamma(C_{rs})$ is the proportion of adequate contacts between a susceptible from a cell C_{pq} and an infective from cells $C_{rs} \in \mathscr{V}_{pq}$.

We define the spatio-temporal distribution of the population based on regions attractiveness by a diffusion term which is parameterized by the potential attractiveness of each cell C_{pq} in the domain Ω as $pot(i, C_{pq})$ and it is given by

$$pot(i, C_{pq}) = \frac{\sum_{j=1}^{F} \alpha_j(C_{pq}, i)}{F} < 1,$$

where $\alpha_j(C_{pq}, i)$ is the number of some attractiveness factors of C_{pq} at time i, and F is the total number of the attractiveness factors. For instance:

$$\begin{aligned}
\alpha_1(C_{pq}, i) &= \frac{\text{Number of hospitals in } c_{pq} \text{ at time i}}{\text{Capacity of hospitals in } c_{pq}} < 1 \\
\alpha_2(C_{pq}, i) &= \frac{\text{Number of accommodation in } c_{pq} \text{ at time i}}{\text{Capacity of accommodation in } c_{pq}} < 1 \\
\alpha_3(C_{pq}, i) &= \frac{\text{Number of educational institutions in } c_{pq} \text{ at time i}}{\text{Capacity of educational institutions in } c_{pq}} < 1 \\
\alpha_4(C_{pq}, i) &= \frac{\text{Number of green spaces in } c_{pq} \text{ at time i}}{\text{Capacity of green spaces in } c_{pq}} < 1 \\
\alpha_5(C_{pq}, i) &= \frac{\text{Number of public transport in } c_{pq} \text{ at time i}}{\text{public transport spaces in } c_{pq}} < 1 \\
\vdots &= \vdots \\
\alpha_F(C_{pq}, i) &= \frac{\text{Number of cultural sector in } c_{pq} \text{ at time i}}{\text{Capacity of cultural sector in } c_{pq}} < 1
\end{aligned}$$

Then, we express the exit of the susceptible, infected and removed individuals from the cell C_{pq} to the attractive neighboring cells $C_{rs} \in \mathscr{V}'_{pq}$ by $-\sum_{C_{rs} \in \mathscr{V}'_{pq}} pot(i, C_{rs}) S_i(C_{pq})$, $-\sum_{C_{rs} \in \mathscr{V}'_{pq}} pot(i, C_{rs}) I_i(C_{pq})$ and $-\sum_{C_{rs} \in \mathscr{V}'_{pq}} pot(i, C_{rs}) R_i(C_{pq})$, respectively. The entry of susceptible, infected and removed individuals to the cell C_{pq} from the neighboring cells $C_{rs} \in \mathscr{V}'_{pq}$ is expressed by $\sum_{C_{rs} \in \mathscr{V}'_{pq}} pot(i, C_{pq}) S_i(C_{rs})$, $\sum_{C_{rs} \in \mathscr{V}'_{pq}} pot(i, C_{pq}) I_i(C_{rs})$ and

$\sum_{C_{rs}\in\mathscr{V}'_{pq}} pot(i,C_{pq})R_i(C_{rs})$, respectively. Based on all theses considerations, the SIR dynamics associated to domain or cell $C_{pq}\in\Omega$ are described based on the following multi-region discrete time model:

$$
\begin{aligned}
S_{i+1}(C_{pq}) &= S_i(C_{pq}) - \sum_{C_{rs}\in\mathscr{V}'_{pq}} pot(i,C_{rs})S_i(C_{pq}) + \sum_{C_{rs}\in\mathscr{V}'_{pq}} pot(i,C_{pq})S_i(C_{rs}) \\
&\quad - \sum_{C_{rs}\in\mathscr{V}_{pq}} \gamma_{pq}(C_{rs})S_i(C_{pq})I_i(C_{rs}) - mS_i(C_{pq}) \qquad (1)\\
I_{i+1}(C_{pq}) &= I_i(C_{pq}) - \sum_{C_{rs}\in\mathscr{V}'_{pq}} pot(i,C_{rs})I_i(C_{pq}) + \sum_{C_{rs}\in\mathscr{V}'_{pq}} pot(i,C_{pq})I_i(C_{rs}) \\
&\quad + \sum_{C_{rs}\in\mathscr{V}_{pq}} \gamma_{pq}(C_{rs})S_i(C_{pq})I_i(C_{rs}) - (m+\rho+\lambda)I_i(C_{pq}) \qquad (2)\\
R_{i+1}(C_{pq}) &= R_i(C_{pq}) - \sum_{C_{rs}\in\mathscr{V}'_{pq}} pot(i,C_{rs})R_i(C_{pq}) + \sum_{C_{rs}\in\mathscr{V}'_{pq}} pot(i,C_{pq})R_i(C_{rs}) \\
&\quad + \lambda I_i(C_{pq}) - mR_i(C_{pq}) \qquad (3)
\end{aligned}
$$

with $S_0^{C_{pq}} > 0$, $I_0^{C_{pq}} > 0$ and $R_0^{C_{pq}} > 0$ are the given initial conditions. $m > 0$ is the natural death rate, $\rho > 0$ is death rate due to the infection, $\lambda > 0$ is the natural recovery rate from infection. A summary of parameters description and values is given in Table 1.

2.2. An optimal control problem. Optimal control theory have proved to be a viable option for the optimization of some variables that influence for instance, the population dynamics of a group of individuals as in the case of epidemics [13, 15, 16, 3, 17, 18].

Optimal control approach have been applied to models (1)-(3) to reduce along the control strategy period, the number of infectious individuals and increase the number of recovered one. For this, we introduce a control variable $u_i^{C_{pq}}$ that characterizes the effectiveness of treatment (vaccination) in the above mentioned model (1-3) associated to the cell $C_{pq}\in\Omega$. Then, the model is given by the following equations:

$$
\begin{aligned}
S_{i+1}(C_{pq}) &= S_i(C_{pq}) - \sum_{C_{rs}\in\mathscr{V}'_{pq}} pot(i,C_{rs})S_i(C_{pq}) + \sum_{C_{rs}\in\mathscr{V}'_{pq}} pot(i,C_{pq})S_i(C_{rs}) \\
&\quad - \sum_{C_{rs}\in\mathscr{V}_{pq}} \gamma_{pq}(C_{rs})S_i(C_{pq})I_i(C_{rs}) - mS_i(C_{pq}) - u_i^{C_{pq}}S_i(C_{pq}) \qquad (4)
\end{aligned}
$$

$$
\begin{aligned}
I_{i+1}(C_{pq}) &= I_i(C_{pq}) - \sum_{C_{rs}\in\mathscr{V}'_{pq}} pot(i,C_{rs})I_i(C_{pq}) + \sum_{C_{rs}\in\mathscr{V}'_{pq}} pot(i,C_{pq})I_i(C_{rs}) \\
&\quad + \sum_{C_{rs}\in\mathscr{V}_{pq}} \gamma_{pq}(C_{rs})S_i(C_{pq})I_i(C_{rs}) - (m+\rho+\lambda)I_i(C_{pq}) \qquad (5)
\end{aligned}
$$

$$
\begin{aligned}
R_{i+1}(C_{pq}) &= R_i(C_{pq}) - \sum_{C_{rs}\in\mathscr{V}'_{pq}} pot(i,C_{rs})R_i(C_{pq}) + \sum_{C_{rs}\in\mathscr{V}'_{pq}} pot(i,C_{pq})R_i(C_{rs}) \\
&\quad + \lambda I_i(C_{pq}) - mR_i(C_{pq}) + u_i^{C_{pq}}S_i(C_{pq}) \qquad (6)
\end{aligned}
$$

The main goal of the control strategy is the minimization of infected individuals and the cost of applying the control in the cell C_{pq}. Then, for an initial state $(S_0(C_{pq}), I_0(C_{pq}), R_0(C_{pq}))$, we consider an optimization criterion associated to cell C_{pq} and we define it by the following objective function

$$
J(u) = \sum_{i=0}^{N} A\, I_i(C_{pq}) + \sum_{i=0}^{N-1} \frac{\tau}{2}(u_i^{C_{pq}})^2 \qquad (7)
$$

where $A > 0$ and $\tau > 0$ are the constant severity weights associated to the number of infected individuals and controls respectively. See the Appendix for more mathematical details.

2.3. Numerical Simulations and Result. In this subsection, we provide numerical simulations to demonstrate our theoretical results in the case when the studied domain represents the assembly of 5^2 cells (regions, cities ...). A code is written and compiled in MATLAB^{TM} using data cited in Table 1 and Fig.1. The optimality systems are solved using an iterative method where at instant i the states $S_i(C_{pq})$, $I_i(C_{pq})$ and $R_i(C_{pq})$ with an initial guess are obtained based on a progressive scheme in time, and their adjoint variables $\zeta_{k,i}^{C_{pq}}$, $k = 1,2,3$, are obtained based on a regressive scheme in time because of the transversality conditions. Afterwards, we update the optimal control values (13) using the values of state and co-state variables obtained in the previous steps. Finally, we execute the previous steps till a tolerance criterion is reached [19, 20, 21, 4, 22, 23].

TABLE 1. Parameters values associated to a cell $C_{pq} \in \Omega$, which utilized for the resolution of all multi-cells discrete-time systems (1)-(3) and (4)-(6), and then leading to simulations obtained from Figure 2 to Figure 10, with the initial conditions $S_0\left(C_{pq}\right), I_0\left(C_{pq}\right)$ and $R_0\left(C_{pq}\right)$ associated to any cell C_{pq} of Ω.

Parameter	Description	Value
$S_0\left(C_{pq}\right)$	Initial value of susceptible	100
$I_0\left(C_{pq}\right)$	Initial value of infected	0
$R_0\left(C_{pq}\right)$	Initial value of removed	0
$\gamma_{pq}(C_{rs})$	Infection transmission rate	1×10^{-5}
m	Natural death rate	1×10^{-4}
λ	Natural recovery rate	2×10^{-5}
ρ	Death rate due to the infection	2×10^{-3}

In order to show the importance of our work, and without loss of generality, we consider here that $M = 5$, and then we present our numerical simulations in a 5×5 grid which represents the global domain of interest. At the initial instant $i = 0$, susceptible people are homogeneously distributed with 100 individuals in each cell except at the lower right corner cell C_{55}, where we introduce 10 infected individuals and 90 susceptible ones.

Regarding the potential attractiveness parameters $pot\left(i, C_{pq}\right)$ for $C_{pq} \in \Omega$, without loss of generality, we chose a fixed value for all the regions of Ω, with the exception of the two regions C_{15} and C_{22} with different values represented in the Fig.1. In all of the figures, the redder part of the color-bars contains larger numbers of individuals, while the bluer part contains smaller numbers.

In the following, we discuss in more detail the cellular simulations we obtain in the case when there is no control yet.

In the Figure 2 we can see that the susceptible population almost vanished after just 500 days, in all parts of that Figure, and the infected one have a maximum raised between 300 and 400 days, while the removed population retains an almost zero value.

FIGURE 1. Potential attractiveness parameters. $pot\left(i,C_{pq}\right)=0.1$ for $C_{pq}\in\Omega$, $pot\left(i,C_{15}\right)=0.4$ and $pot\left(i,C_{22}\right)=0.2$.

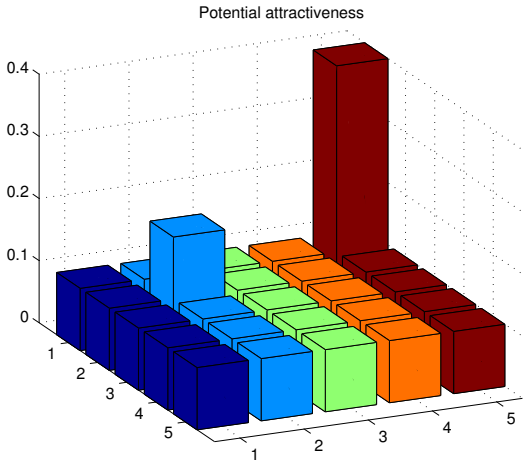

FIGURE 2. Susceptible, infected and removed populations behavior in the absence of control. (a) The populations $S\left(C_{pq}\right)$, $I\left(C_{pq}\right)$ and $R\left(C_{pq}\right)$ in the cell $C_{pq}\in\Omega\backslash\{C_{51},C_{22}\}$ where $pot\left(i,C_{pq}\right)=0.1$. (b) The populations $S(C_{15})$, $I(C_{15})$ and $R(C_{15})$ in the cell C_{15} where $pot\left(i,C_{pq}\right)=0.4$. (c) The populations $S(C_{22})$, $I(C_{22})$ and $R(C_{22})$ in the cell C_{22} where $pot\left(i,C_{pq}\right)=0.2$.

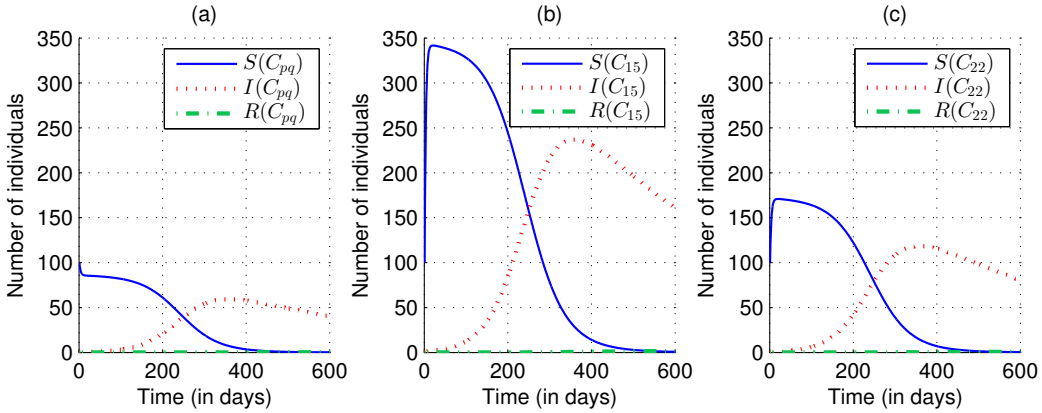

Figure 2 depicts the impact of the city attractiveness, while in cells $C_{pq}\in\Omega\backslash\{C_{51},C_{22}\}$ (a), the number of the susceptible population decreases continuously from 100 to almost zero. While in the other most attractive cities, the number of susceptibles increases rapidly at the beginning up to a maximum value of 345 individuals in cell C_{15} (b) and 170 individuals in cell C_{22} (c) ,

FIGURE 3. Susceptible and infected populations at several instants. **The four upper sub-figures:** The population $S\left(C_{pq}\right)$ where $C_{pq} \in \Omega$, from i=0 to i=600. **The four lower sub-figures:** The population $I\left(C_{pq}\right)$ where $C_{pq} \in \Omega$, from i=0 to i=600.

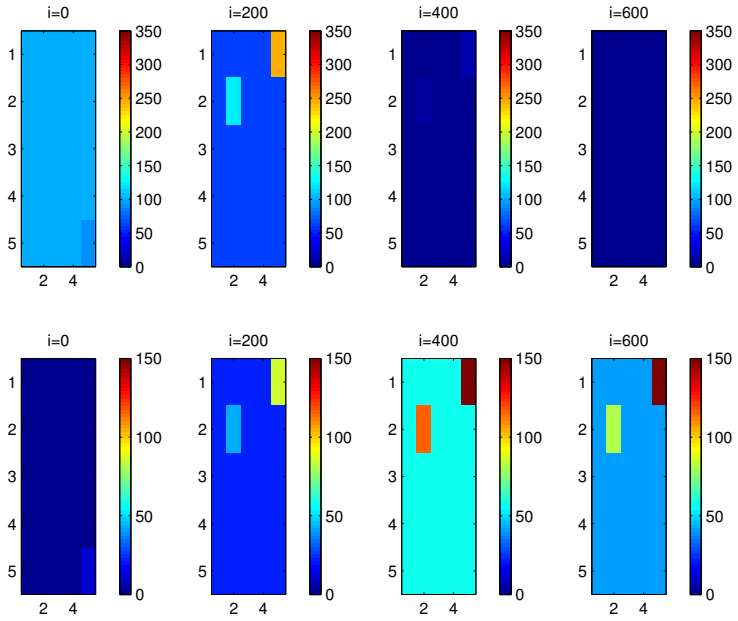

and then began to decrease to zero. In all remaining cells C_{pq} (a), the maximum value of the susceptible population does not exceed 100 individuals, and the infected one dose not exceed 60 individuals, compared to the number of the infected population in the most attractive cities that reaches 240 individuals in C_{15} and 120 individuals in C_{22}.

Figure 3 depicts the evolution of the epidemic within Ω with respect to the susceptible population (The upper four sub-figures) and the infected one (The lower four sub-figures), we have neglected the removed population because it retains an insignificant value. As it shown in this Figure, the epidemic have started from the lower right corner at instant i=0. Note that in the top four sub-figures (susceptibles), the colorbar has a maximum value equal to 350, while in the four down sub-figures (infectives), it has just 150.

At instant i=0, 100 susceptible were distributed in each cell of Ω, except the lower right corner cell in which just 90 ones. At instant i=200, it can be seen that all cells have begun to lose their susceptible population, except the most attractive regions (C_{22} and C_{15}) which keep more than 200 individuals in the susceptible group of C_{15} and 125 individuals in C_{22}. At instants

FIGURE 4. The susceptible, infected and the removed populations after use of the vaccination control . (a). The populations $S(C_{43})$, $I(C_{43})$ and $R(C_{43})$ in the cell C_{43} in which the vaccination control is introduced. (b) The populations $S(C_{15})$, $I(C_{15})$ and $R(C_{15})$ in the cell C_{15}. (c) The populations $S(C_{22})$, $I(C_{22})$ and $R(C_{22})$ in the cell C_{22}. (d) The populations $S\left(C_{pq}\right)$, $I\left(C_{pq}\right)$ and $R\left(C_{pq}\right)$ in the cell $C_{pq} \in \Omega \backslash \{C_{51}, C_{22}, C_{43}\}$

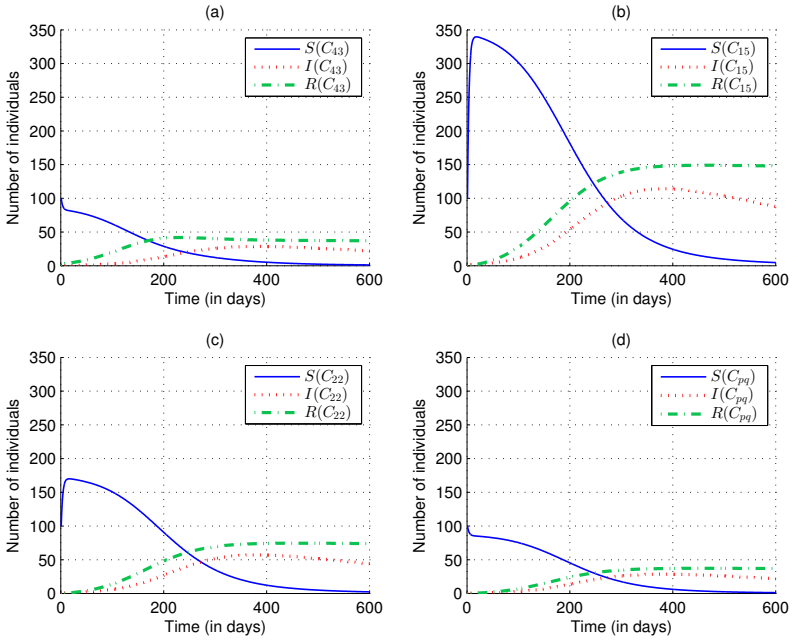

i=400 and i=600, all the susceptible individual almost vanished with some delay in cells C_{22} and C_{15}.

Regarding the infected population, in the down sub-figures, we can see that at the first there is no infection in all cells of Ω, except the lower right corner cell in which there is 10 infected individuals. At instant i=200, the number of infections began to increase continuously, while cells C_{22} and C_{15} attract more infected individuals and quickly the number of infections becomes enormous. From instant i=400 to instant i=600, the number of infections reach its maximum and began to decrease, but in the attractive regions, the number of infections keeps a value more than 150 in the cell C_{15}, and more than 70 in the cell C_{22}.

Figure 4 depicts the several populations after use of the vaccination control in the cell C_{43} (a) in which the number of removed individuals rise to almost 50 individuals at instant i=170,

and almost 45 removeds in the other cells of Ω, compared to the zero value of removeds before the use of control. The most important remark that can be extracted from this figure is that the number of the removed population in the most attractive regions reaches an unexpected value, where in the cell C_{15} the number of removeds exceeds 150 removeds, and 70 ones in the cell C_{22}, while this number does not leave zero before the control.

The Figure 4 shows the important role of vaccination control in reducing the number of infections in all parts of Ω, while in cell C_{43} the number of infected individuals does not exceed 40, compared to 60 infected before use of the control (see Figure 1 (a)). Before using the control of vaccination, the number of infected in the attractive regions reached a maximum value of about 240 infections in C_{15} and 120 infections in C_{22}, while after the use of control, the number of infected individuals is still less than 120 in C_{15} and less than 70 in the cell C_{22}.

Compared with the results of [19, 20], it can be seen that when considering the attractiveness of regions, more efficient results can be obtained, as can be seen from Figure 4 (d). The number of removeds becomes greater than the number of infections in a region not controlled. This confirms the positive influence of one region on the other [19, 20, 21, 23, 22], with which the control objective can be achieved with minimal cost, by introducing a vaccination control in a single region among several others and maximizing the size of the removed population while minimizing the number of infections in all parts of the area of interest.

While in the Figure 3, the removed population is neglected because of the almost zero value that has, Figure 5 depicts the efficiency of vaccination control in reducing the infected population and increasing the removed one in all regions of Ω. While before the use of the control the simulation associated to the removed population contains just the blue color in all parts of Ω, for that reason this Figure is not incorporated (neglected).

The vaccination control is used just in the cell C_{43} and we can see that number of the removed individuals in the more attractive regions takes a very huge values compared to the cell C_{43}, and this is a very interesting result, where an uncontrolled region reaches the objective of maximizing its removed population and minimizing its infected one, based only on its potential attractiveness.

FIGURE 5. Susceptible, infected and removed populations at several instants. **The four upper sub-figures:** The population $S\left(C_{pq}\right)$ where $C_{pq} \in \Omega$, from i=0 to i=600. **The four middle sub-figures:** The population $I\left(C_{pq}\right)$ where $C_{pq} \in \Omega$, from i=0 to i=600. **The four lower sub-figures:** The population $R\left(C_{pq}\right)$ where $C_{pq} \in \Omega$, from i=0 to i=600.

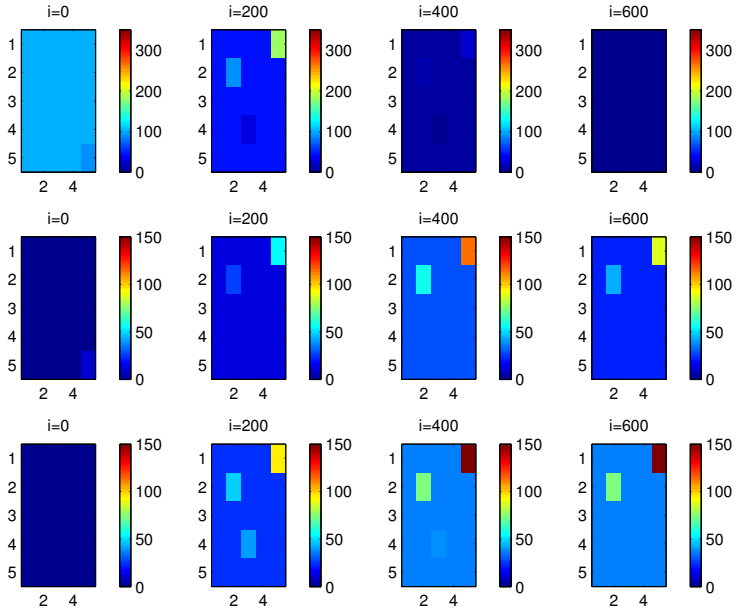

It is clear that at the instant i = 400 and i = 600 in the two Figures 3 And 5, infection in the most attractive regions retains a high value which is represented by the redder color in the four lower sub-figures of the Figure 3, compared with a smaller value of infected individuals in the middle four sub-figures of the Figure 5, which is represented by the orange color as the maximum value in the cell C_{15} at instant i=400, and the yellow color as the maximum at instant i=600.

The comparison of the susceptible populations after and before the use of the vaccination control is evident, and it can be deduced from the both Figures 3 And 5, at the instant i=200, that after use of the control, the susceptible population is reduced compared to the case when there is no control.

In Figure 6 we can see the impact of the potential attractiveness parameters on the different populations $S\left(C_{43}\right)$ in (a), $I\left(C_{43}\right)$ in (b) and $R\left(C_{43}\right)$ in (c). The solid line in blue represents the

FIGURE 6. The impact of the potential attractiveness parameter $pot\,(i,C_{43})$ on the control efficiency. (a) The population $S(C_{43})$ with different values of the parameter $pot\,(i,C_{43})$. (b) The population $I(C_{43})$ with different values of the parameter $pot\,(i,C_{43})$. (c) The population $R(C_{43})$ with different values of the parameter $pot\,(i,C_{43})$.

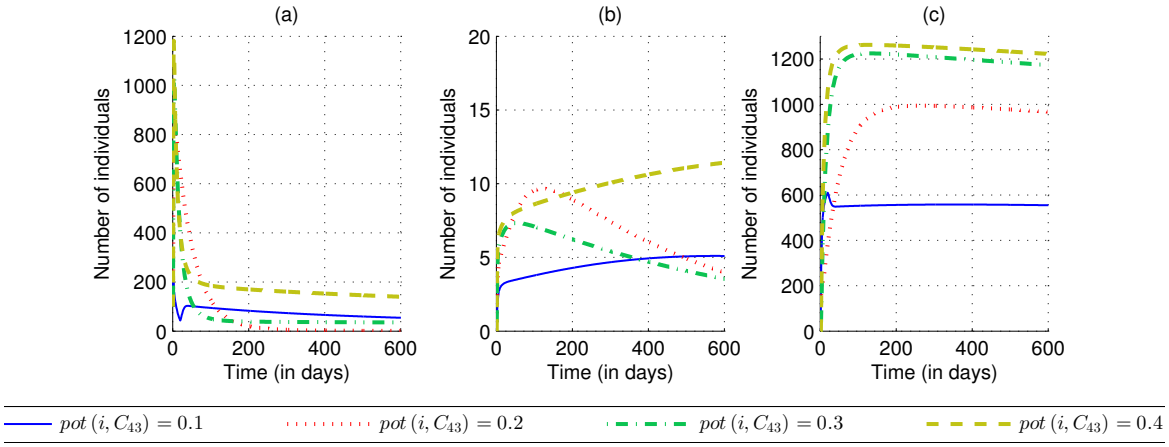

first case ($pot\,(i,C_{43}) = 0.1$) presented above (see Figure 4 in (a)) but in Figure 6, populations are separated. This case is presented here for a better comparison.

It is clear from this Figure that there is no adjustment between the potential attractiveness parameter and the number of susceptibles and/or infectives and/or removeds, which means that if this parameter is large, this does not imply that the number of susceptible (infectives or removeds) persons is also large. As can be seen in Figure 6 (a), the blue line is over the green one, which means that if the controlled region is more attractive, the number of susceptibles may decrease and then increase, depending on the severity of attractiveness.

We can see that in the case of $pot\,(i,C_{43}) = 0.2$ all susceptibles are disappear after just 200 days while the number of susceptibles retains a non zero values in the other cases (Figure 6 (a)).

From the sub-figure (b) in this same Figure, we can see clearly that the case when $pot\,(i,C_{43}) = 0.3$ (the green line) is the better one, where the number of infections takes the smaller value after 400 days decreasing to zero. The second case is the case when $pot\,(i,C_{43}) = 0.2$ where the number of infections also converges to zero after an increase of

9 cases of infections. When $pot\,(i, C_{43}) = 0.4$ the number of infected people increases continuously exceeding 10 cases of infection

Figure 6 (c) depicts the agreement between the potential attractiveness parameter and the size of the removed population, it is clear that if the more this parameter is big, the size of the removed population is more big.

The very important idea that can be extracted from these figures is that in order to control a region connected with several other regions by any kind of anthropological movement, it is necessary to consider the impact of the potential attractiveness parameter, to ensure good control results.

3. Case Study: Application to the Grand Casablanca-Settat Region

3.1. Presentation of the studied region (Grand Casablanca-Settat). We chose the Grand Casablanca-Settat region as the studied region in this paper because we are convinced that we can find some useful data to support our work. It is the most populated and dynamic region of Morocco, that contains Casablanca city as the economic and industrial capital of Morocco because with its demographic growth and continuous development of the industrial sector [25], and 167 other provinces and communes (see Fig. 7). Which allows us to illustrate the objective of our research. Figure 7 illustrates an example of discrete geographical domains of region of Casablanca-Settat (Morocco) where $p = 168$, that image was originally made based on information from [24].

3.2. The potential attractiveness. The concept of attractiveness has become a very interesting field of research in population dynamics not only for humans, but also for animals, birds and even mosquitoes. Where billions of animals, including mammals, fish, insects and birds, travel long distances to track seasonal changes in resources and habitats[26]. Generally, fish migration is characterized by active displacement among very different structures (fresh water, salty waters, for example)[27], On the other hand, the spatial distribution of Cattle Heron is closely related to environmental factors such as the availability of food resources [28]. In most cases, hunting can influence the spatial and temporal distribution of birds and fish. Birds disturbed by hunting should therefore move from hunting sites to prohibited sites [29]. Even insects can

FIGURE 7. Region of Casablanca-Settat in Morocco. This region is divided into 168 sub-regions (or communes) $(\Omega_i)_{1\leq i\leq 168}$, each commune with its population is given in the following table based on data from [24].

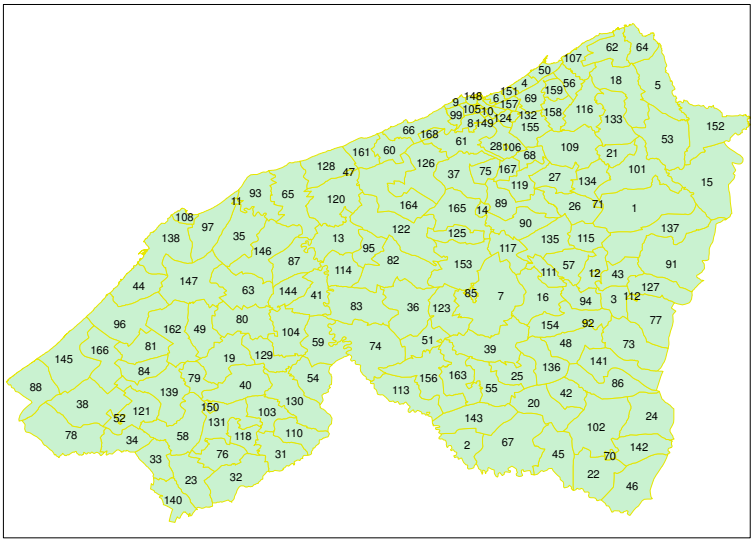

Nb	Name	Population	Nb	Name	Population	Nb	Name	Population	Nb	Name	Population
1	Ahlaf	11451	43	Sidi Dahbi	8703	85	Settat (Mun.)	142250	127	Lakhzazra	8582
2	Ain Blal	4699	44	Sidi Abed	22980	86	Sgamna	10245	128	Lamharza Essahel	17766
3	Ain Dorbane-Lahlaf	8120	45	Sidi Ahmed El Khadir	9687	87	Si Hsaien Ben Abderrahmane	5990	129	Laamria	10520
4	Ain Harrouda (Mun.)	62420	46	Laqraqra	11419	88	Loualidia	18616	130	Laaounate	17850
5	Ain Tizgha	15692	47	Lbir Jdid (Mun.)	24136	89	Jaqma	10306	131	Laatatra	17593
6	ARn-Seban (Arrond.)	171452	48	Mniaa	11789	90	Lambarkiyine	8559	132	Tit Mellil (Mun.)	32782
7	Mzamza Janoubia	20802	49	Mogress	15705	91	Oulad M'Hamed	10187	133	Oulad Yahya Louta	9430
8	ARn-Chock (Arrond.)	377744	50	Mohammadia (Mun.)	208612	92	Oulad M'Rah (Mun.)	8697	134	Rdadna Oulad Malek	4561
9	Anfa (Arrond.)	94504	51	Khemisset Chaouia	5527	93	Sidi Ali Ben Hamdouche	35182	135	Riah	8373
10	Assoukhour Assawda (Arrond.)	115704	52	Zemamra (Mun.)	13279	94	Oued Naanaa	6991	136	Rima	8949
11	Azemmour (Mun.)	40920	53	Ziaida	14581	95	Oulad Abbou (Mun.)	11299	137	M'Garto	8514
12	Ben Ahmed (Mun.)	33105	54	Bni Tsiriss	14067	96	Oulad Aissa	23370	138	My Abdellah	74671
13	Ben Maachou	8458	55	Bni Yagrine	13031	97	Haouzia	28821	139	Saniat Berguig	28854
14	Berrechid (Mun.)	136634	56	Bni Yakhlef	48338	98	Hay Mohammadi (Arrond.)	138760	140	Oulad Amrane	12252
15	Bir Ennasr	4855	57	Bouguargouh	9539	99	Hay-Hassani (Arrond.)	468542	141	Oulad Fares	12341
16	Ras El Ain Chaouia	14747	58	Bouhmame	23234	100	Mechouar de Casablanca (Mun.)	2645	142	Oulad Fares El Halla	3021
17	Ben M'Sick (Arrond.)	131883	59	Boulaouane	14485	101	Mellila	15081	143	Oulad Freiha	11581
18	Benslimane (Mun.)	57101	60	Soualem Trifiya	33079	102	Meskoura	7180	144	Ouled Frej	19752
19	Bni Hilal	17843	61	Bouskoura (Mun.)	103026	103	Metrane	10580	145	Ouled Ghanem	24775
20	Bni Khloug	12930	62	Bouznika (Mun.)	37238	104	Mettouh	25856	146	Oulad Hamdane	11577
21	Oulad Ali Toualaa	5504	63	Chaibate	9877	105	El Maarif (Arrond.)	170689	147	Ouled Hcine	32130
22	Oulad Amer	6673	64	Charrate	9754	106	Mediouna (Mun.)	22442	148	Sidi Belyout (Arrond.)	189715
23	Koudiat Bni Dghough	15181	65	Chtouka	33170	107	El Mansouria (Mun.)	19853	149	Sbata (Arrond.)	116255
24	Oulad Bouali Nouaja	6507	66	Dar Bouazza (Mun.)	151373	108	El Jadida (Mun.)	194934	150	Sidi Bennour (Mun.)	55815
25	Guisser	12289	67	Dar Chaffai	17454	109	Moualine El Oued	9129	151	Sidi Bernoussi (Arrond.)	173189
26	Ouled Cebbah	7606	68	Deroua (Mun.)	47719	110	Oulad Boussaken	7390	152	Sidi Bettache	6927
27	Ouled Zidane	6434	69	Ech-challalate	53503	111	Oulad Chbana	8081	153	Sidi El Aidi	13839
28	Al Majjatia Oulad Taleb	32286	70	El Borouj (Mun.)	19235	112	Loulad (Mun.)	6057	154	Sidi Hajjaj	20732
29	Al-Fida (Arrond.)	158667	71	El Gara (Mun.)	20855	113	Machraa Ben Abbou	9355	155	Sidi Hajjaj Oued Hassar	20349
30	Mers-Sultan (Arrond.)	129759	72	Moulay Rachid (Arrond.)	245484	114	Sidi Abdelkhaleq	6122	156	Sidi Mohammed Ben Rahal	10410
31	Khmis Ksiba	5665	73	Mrizigue	8376	115	Sidi Abdelkrim	14037	157	Sidi Moumen (Arrond.)	454779
32	Tamda	9750	74	Mzoura	9525	116	Fdalate	11966	158	Sidi Moussa Ben Ali	11445
33	Kridid	14351	75	Nouaceur (Mun.)	23802	117	Foqra Oulad Aameur	6256	159	Sidi Moussa Majdoub	20330
34	Laagagcha	13748	76	M'Tal	9913	118	Jabria	19676	160	Sidi Othmane (Arrond.)	220047
35	Oulad Rahmoune	28449	77	N'Khila	12306	119	Kasbat Ben Mchich	14905	161	Sidi Rahal Chatai (Mun.)	20628
36	Oulad Said	9271	78	Lgharbia	22729	120	Laghdira	19973	162	Sidi Smail	28733
37	Oulad Salah	15031	79	Lmechrek	16141	121	Laghnadra	33553	163	Toualet	11976
38	Oulad Sbaita	25650	80	Zaouiat Lakouacem	10967	122	Laghnimyine	17513	164	Had Soualem (Mun.)	36765
39	Oulad Sghir	13866	81	Zaouiat Saiss	11160	123	Lahouaza	7394	165	Sidi El Mekki	8920
40	Oulad Si Bouhya	18198	82	Zaouiat Sidi Ben Hamdoun	9521	124	Lahraouyine (Mun.)	64821	166	Sidi M'Hamed Akhdim	10817
41	Oulad Sidi Ali Ben Youssef	10032	83	Gdana	9084	125	Lahsasna	9315	167	Oulad Ziyane	17095
42	Sidi Boumehdi	5081	84	Sebt Saiss	10488	126	Sahel Oulad H'Riz	38156	168	Oulad Azzouz	40372

be attracted to other places to escape deteriorating habitats, colonize new places and/or to find temporary shelter, such as winter sites [30].

In general, the potential attractiveness of animals does not have as many factors as humans. Sometimes it can be the same, such as in wars, natural disasters ... . But usually human has more and more requirements, hospitals, green spaces, beaches, schools, public transportation, public directions ....

3.3. The potential attractiveness model. In order to set up a qualitative model for mapping the potential attractiveness in the Grand Casablanca-Settat region, we opted for a qualitative method based on the use of topographic data as well as observations made in the field using the ArcGIS Geoprocessing Tool. Without lose of generality, we chose as potential attractiveness factors in the Grand Casablanca-Settat region, only factors that are available on data, then representative point maps have been created for each of these entities:

- Hospitals : Peripheral hospitals and university hospitals
- Higher institutions: It represents faculties, colleges, institutes, and engineering schools
- Industrial zones: Factories, ports, companies .
- Touristic places: Hotels, Some worth seeing places.

From Google Maps, we retrieved the representative points of each entity described above manually, the points collected are all in WGS 84 coordinate system, these data were imported into Arcgis to create four layers, first layer for hospitals, the second for higher institutions, another for industrial zones and the last for touristic places.

In a second step we transformed each layer dots into a polygon layer, creating a buffer zone at a given distance from the input entities (5km for industrial zones , 3km for hospitals, higher institutions and touristic places).

The third step is the conversion of the result into a raster carrying two values: the value 0 for the non-attractive zone and 1 for the attractive zone. In order to produce the map of the most attractive places, the overlay tool was used in the fourth and last step in the ArcGIS environment. This tool involves one of the most widely used approaches to solve multi-criteria problems, thus the calculation of the potential attractiveness in the Grand Casablanca-Settat region. The

FIGURE 8. Methodological flowchart.

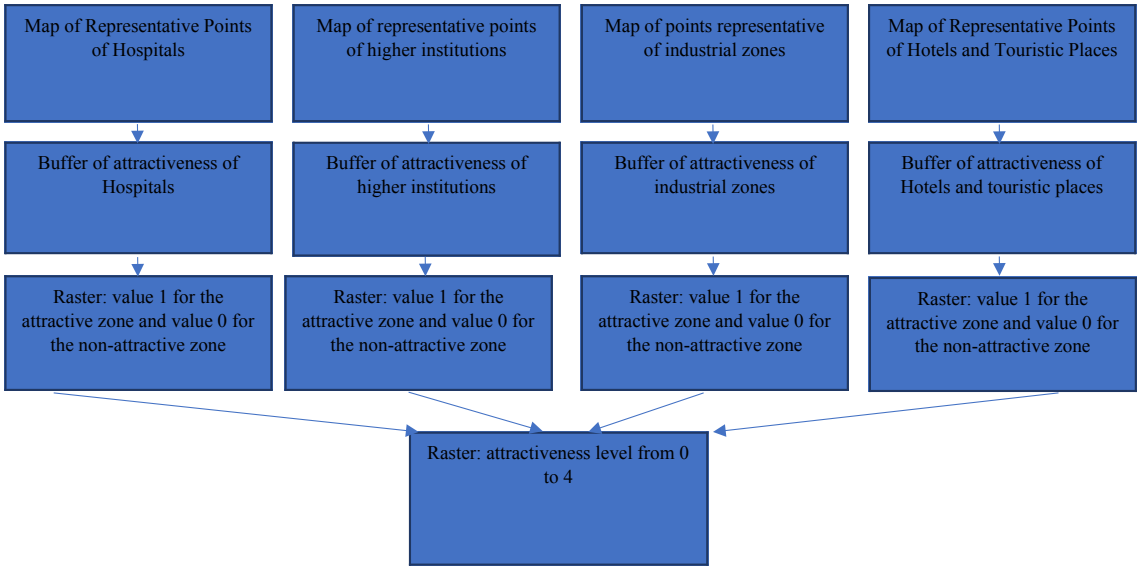

calculation was made by using the tool 'Map algebra' which allowed to add the four layers to result in the level of attractiveness of each place. The formula used is the following:

$$At = Hp + Hi + Iz + Tp \tag{8}$$

Where At is the attractiveness level, Hp is the potential attractiveness of Hospitals, Hi is the potential attractiveness of Higher institutions, Iz is the potential attractiveness of Industrial zones and Tp is the potential attractiveness of Touristic places. Fig. 8 summarizes all above steps of the creation of the potential attractiveness map in Grand Casablanca-Settat region.

3.4. Construction of the attractiveness map.

3.4.1. *Higher Education Institutions:* Higher Education Institutions (HEI) in Grand Casablanca-Settat region include public and private faculties, schools, institutes and multidisciplinary vocational training centers. HEI attract a large number of students, towards a zone of influence which we have supposed of radius 3 Km. Then we created a map to visualize the attractive zones of HEI in the Grand Casablanca-Settat region (See (a) of Fig. 9).

3.4.2. *Industrial zones:* Work displacements play an essential role in the structure of the environment [31]. A study in France showed that in 1999, three out of five workers worked outside

FIGURE 9. (a) Institutions of higher education in Grand Casablanca-Settat region. (b) Industrial zones in Grand Casablanca-Settat region.

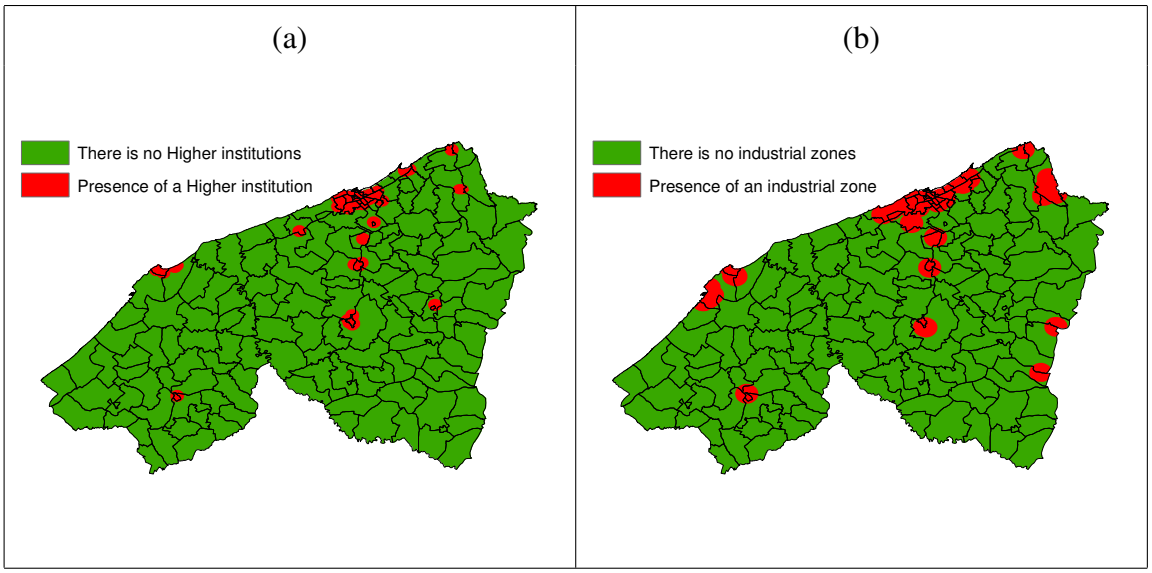

their municipality of residence, this flow of home-work mobility results in a high concentration of jobs in urban centers [32]. The mobility flow caused by the industrial areas is very important, and it is assumed that the area of influence of such kind of factors is within 5 km of the center of each entity. The reason behind choosing 5 km for industrial zones is that most of workers try to find closer places to live, but small and large companies and factories can employ a huge number of workers, which means that the attracted population occupies a wide area compared to the other factors (See (b) of Fig. 9).

3.4.3. *Hospitals.* Hospitals are the main pillars of the health chain, capable of provoking a particularly pronounced polarization in the flow of displacement that it generates within a municipality [33]. In our data, we consider as an attractive hospital only the big ones, that have all the sanitary equipment makes it a complete and independent unit. The specialized units of Casablanca University Hospital welcome patients not only from Casablanca, but from all over the Kingdom, but we suppose that hospitals attractiveness area is within 3 km. Hospitals form a strong attractiveness factor (See (a) of Fig. 10).

3.4.4. *Touristic Places:* A tourist has been defined by the World Tourism Organization as being an individual present at least one night in a site of reception out of his home, by motivations

FIGURE 10. (a) Hospitals in Grand Casablanca-Settat region. (b) Touristic places in Grand Casablanca-Settat region.

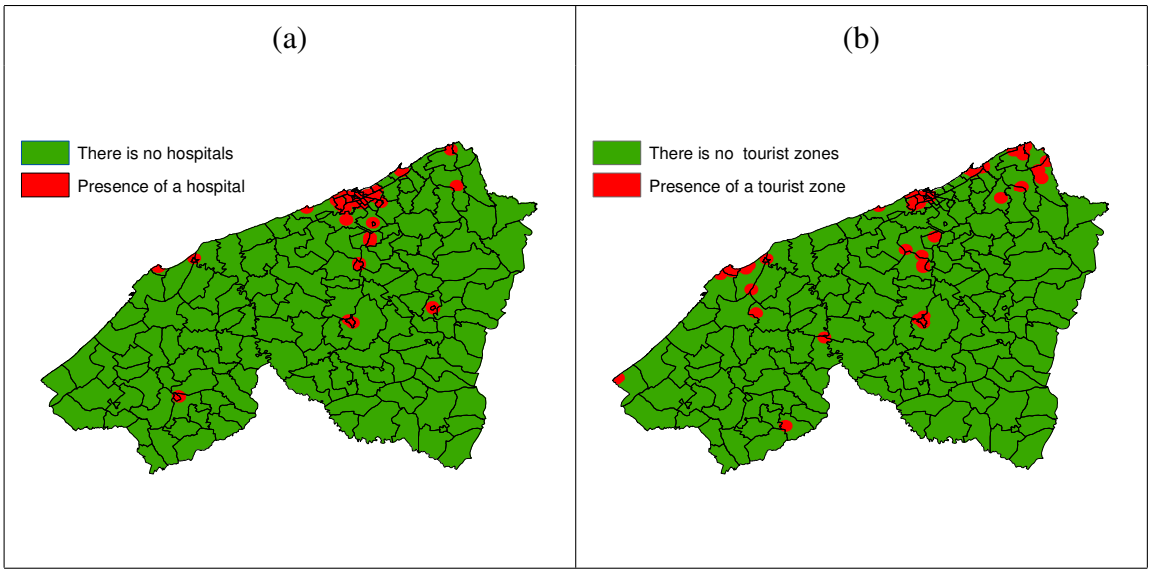

possibly pertaining to relaxation and holidays leisure. The tourist attractiveness is associated with the destination and features such as the atmosphere of the site, the services offered, the affordability ...[34]. In this part of the paper, hotels and some worth seeing places (Hassan II Mosque, some green spaces, El Jadida beach...) are considered as the tourist attractiveness factor (See (b) of Fig. 10).

3.5. The map of the potential attractiveness in Grand Casablanca-Settat: The ArcGIS software allowed us to overlay the four previous layers. The results will be illustrated by thematic maps that allow to visualize the most attractive places in the Grand Casablanca-Settat region, see Fig. 11. From that figure we can see the different zones of attractiveness all over the region, not only in Casablanca as expected. There are more than 8 poles of attractiveness, defined only by 4 factors, HEI, Industrial zones, hospitals and touristic places.

These poles influence economic mobility, anthropological distribution, the development of agriculture and more. This results can be used to simplify the implementation of control strategies, the organization of cultural events and the implementation of awareness campaigns.

3.6. The effect of regions attractiveness on epidemics outbreak: Here we consider an hypothetical epidemic that spreads in the Grand Casablanca-Settat region by starting from

FIGURE 11. The potential attractiveness map in Grand Casablanca-Settat region.

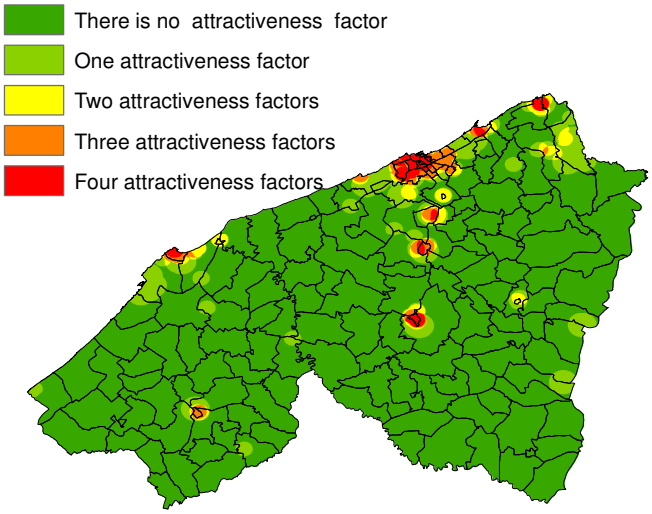

Berrechid (Mun) at the initial time $i = 0$ with 100 infected individuals, and all the other regions are considered as susceptible population. Based on the potential attractiveness map carried out in the previous subsection, we extract the diffusion term of each zone, then we incorporate them with parameters values from Table 1 to simulate the spread of that epidemic in the Grand Casablanca-Settat region.

The dynamic of the model (1)-(3) is depicted in figures 12, 13 and 14, while the figures 15, 16 and 17 depict the controlled model (4)-(6). In this simulations we consider four time steps, that is $i = 0$ (Top right), $i = 100$ (Top left), $i = 200$ (Bottom right) and $i = 300$ (Bottom left).

In Fig.12, we can see the global diffusion of susceptible people in the whole studied area, but after some time it can be seen that the susceptible population decreases especially in the most attractive regions such as in the Casablanca city. From Fig.13, it can be seen that the infected population increases and spreads out all over the most attractive regions. In Fig.14, we can see that the removed population increases very slowly and it remains very limited.

From these simulations, it can be seen that the infection spread out to the nearest attractive zones. That is the infection starts from Berrechid (Mun) to Nouaceur (Mun.) and then to Casablanca city. This fact explains why the infection spread northward from the coast and why it did not reach the south west even there are some attractive zones.

FIGURE 12. Susceptible individuals without control strategy in the Grand Casablanca-Settat region.

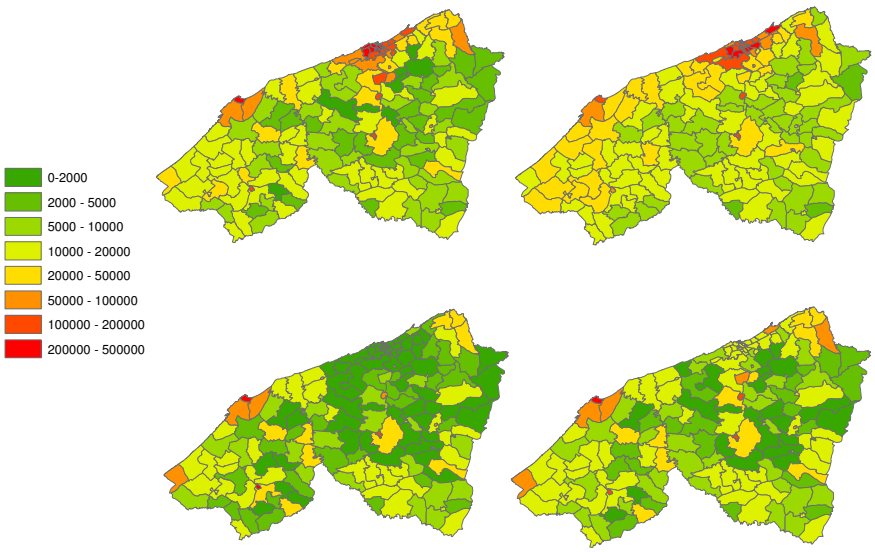

These simulations give an idea of the probable direction of the spread of epidemics by considering the attractiveness of the regions. Thus, results of that paper can be used by the decision makers to identify and track the evolution of epidemics within a more complex system of connected zones.

In Fig.15, we can see the diffusion of the susceptible population under control strategy which is applied in the source of infection that is Berrechid (Mun). The susceptible population is also decreased but it remains more important compared to the case when there is no control. From Fig.16, it can be seen that the infected population reaches small numbers compared to the case when there is no control (Fig.13). Infected people also spread to all the nearest attractive areas, but with a small number of people.

Fig.17 depicts the diffusion of the removed population where it can be seen that the removed individuals reach big numbers in all the nearest attractive zones, compared to the case of Fig.14 when there is no control strategy.

FIGURE 13. Infected individuals without control strategy in the Grand Casablanca-Settat region.

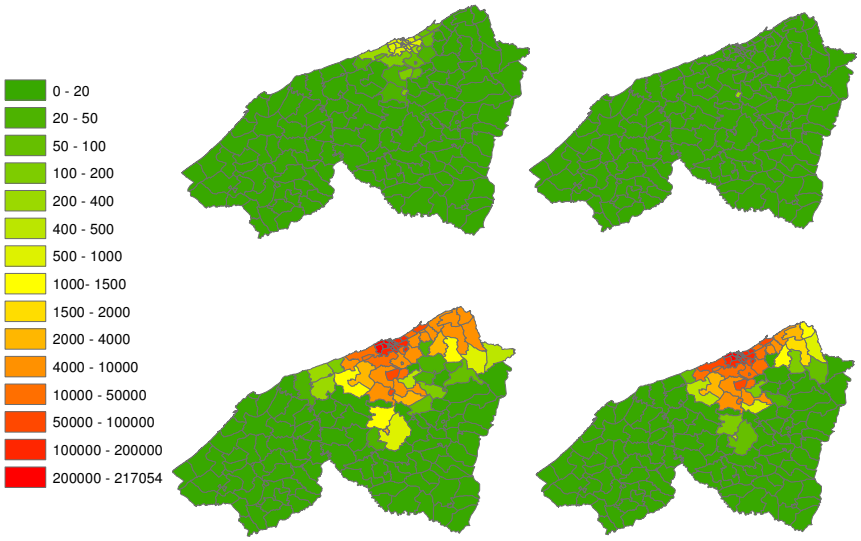

FIGURE 14. Removed individuals without control strategy in the Grand Casablanca-Settat region.

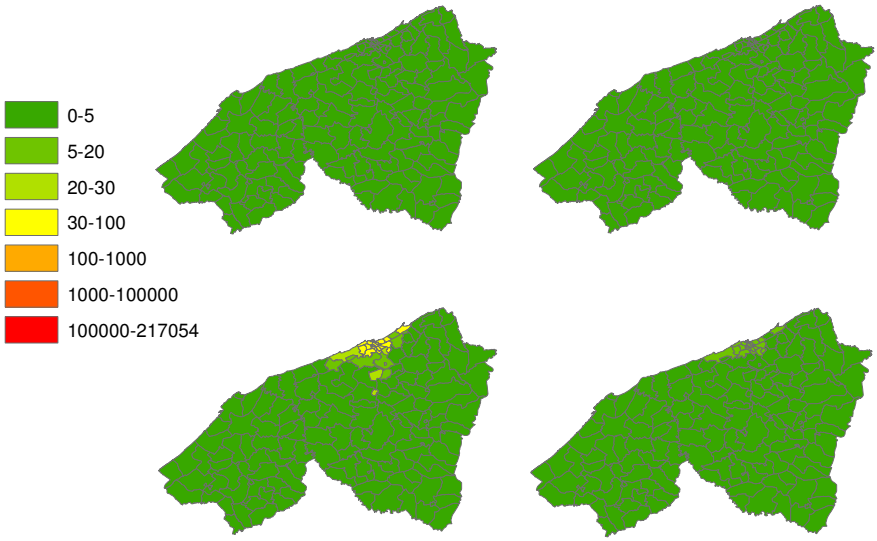

FIGURE 15. Susceptible individuals with control strategy in the Grand Casablanca-Settat region.

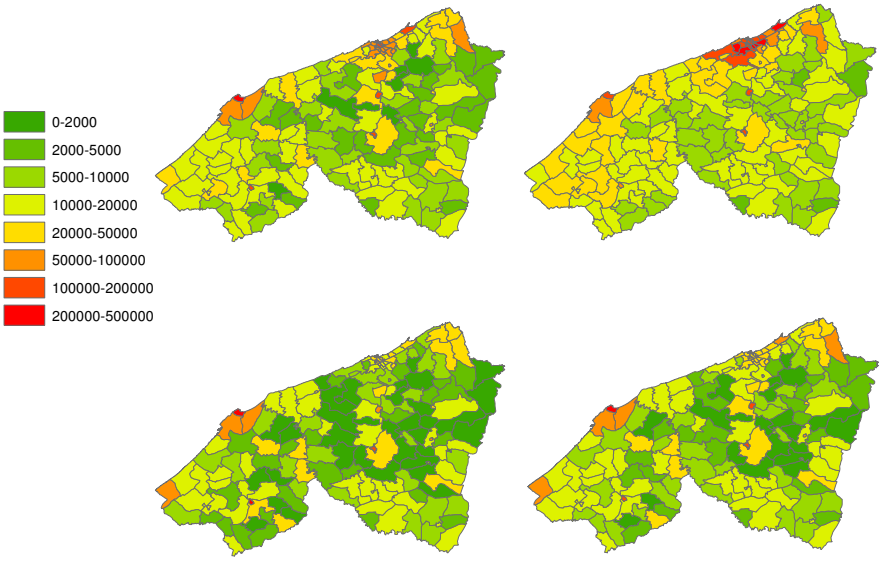

FIGURE 16. Infected individuals with control strategy in the Grand Casablanca-Settat region.

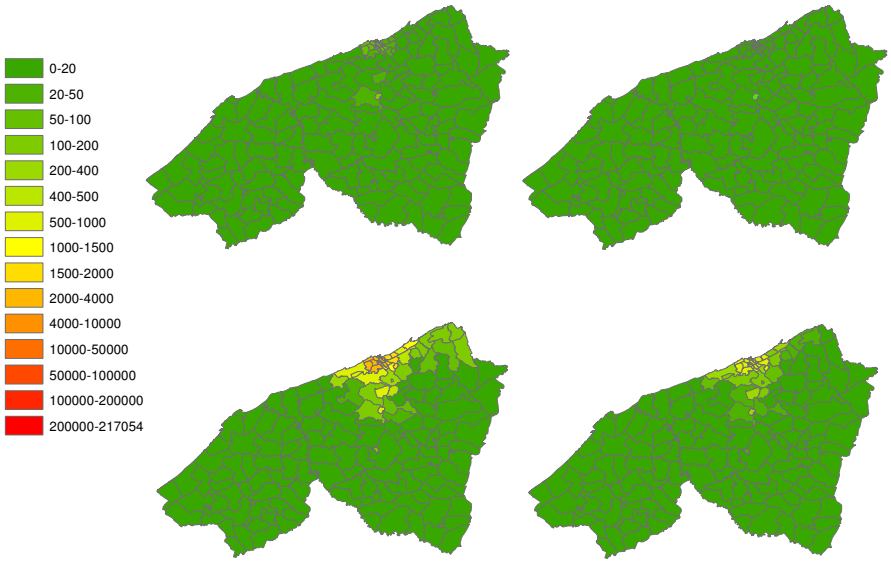

FIGURE 17. Removed individuals with control strategy in the Grand Casablanca-Settat region.

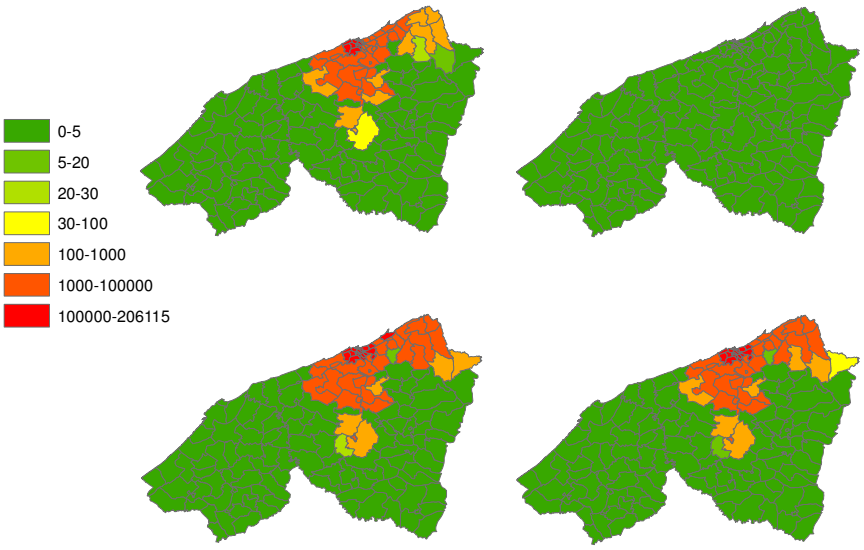

4. CONCLUSION

In this paper, we have generalized a discrete time multi-regions SIR epidemic model proposed in [19, 20], in which we defined and introduced a new potential attractiveness parameters of regions. Our results show that the most attractive regions get more infections than the others and there is no proportionality between these parameters and the susceptible population size. An optimal control is also investigated to characterize the treatment (vaccination) which allows to reduce the infectious individuals and increase the number of recovered ones in a region with varying potentials and this with an optimal cost. A discrete version of Pontryagin's maximum principle is done to analyze the optimal control problem. The potential attractiveness parameters play a very interesting role in the control of connected regions, where the most attractive regions reach the control objective based only on the positive influence of regions. Numerical simulations with several scenarios are given to illustrate and discuss theoretical results. Finally, we applied our results to study the spread of infection within the Grand Casablanca-Settat region after determining the attractiveness map based on data originally collected and analyzed

with the powerful ArcGis tools. Results of that paper can be used by the decision makers to identify and track the evolution of epidemics within a more complex system of connected zones.

APPENDIX

In the optimal control problem that we consider in this paper, our interest is the minimization of the objective function given by (7) subject to system (4)-(6). In the other word, we are seeking an optimal control $u = (u_i^{C_{pq}})_{i=0,\dots,N-1}$ such that

$$J(u) = \min\{J(u) \mid u \in \mathscr{U}_{ad}\} \tag{9}$$

Where $\mathscr{U}_{ad}$ is the set of admissible controls defined by

$$\begin{aligned} \mathscr{U}_{ad} &= \{u = (u_i^{C_{pq}})_{0\le i\le N-1} \mid \\ &\quad u_{min} \le u_i^{C_{pq}} \le u_{max},\ 0 \le i \le N-1\}. \end{aligned}$$

The sufficient condition for existence of an optimal control for the problem follows from theorem 1 in [16]. At the same time by using Pontryagin's Maximum Principle [35] we derive necessary conditions for our optimal control problem. For this purpose we define the Hamiltonian as:

$$\begin{aligned} \mathscr{H}(\Omega) &= A\, I_i(C_{pq}) + \frac{\tau}{2}(u_i^{C_{pq}})^2 \\ &+ \zeta_{1,i+1}^{C_{pq}} \Bigg[S_i(C_{pq}) - \sum_{C_{rs}\in\mathscr{V}'_{pq}} pot(i,C_{rs}) S_i(C_{pq}) + \sum_{C_{rs}\in\mathscr{V}'_{pq}} pot(i,C_{pq}) S_i(C_{rs}) \\ &\quad - \sum_{C_{rs}\in\mathscr{V}_{pq}} \gamma_{pq}(C_{rs}) S_i(C_{pq}) I_i(C_{rs}) - m S_i(C_{pq}) - u_i^{C_{pq}} S_i(C_{pq}) \Bigg] \\ &+ \zeta_{2,i+1}^{C_{pq}} \Bigg[I_i(C_{pq}) - \sum_{C_{rs}\in\mathscr{V}'_{pq}} pot(i,C_{rs}) I_i(C_{pq}) + \sum_{C_{rs}\in\mathscr{V}'_{pq}} pot(i,C_{pq}) I_i(C_{rs}) \\ &\quad + \sum_{C_{rs}\in\mathscr{V}_{pq}} \gamma_{pq}(C_{rs}) S_i(C_{pq}) I_i(C_{rs}) - (m+\rho+\lambda) I_i(C_{pq}) \Bigg] \\ &+ \zeta_{3,i+1}^{C_{pq}} \Bigg[R_i(C_{pq}) - \sum_{C_{rs}\in\mathscr{V}'_{pq}} pot(i,C_{rs}) R_i(C_{pq}) + \sum_{C_{rs}\in\mathscr{V}'_{pq}} pot(i,C_{pq}) R_i(C_{rs}) \\ &\quad + \lambda I_i(C_{pq}) - m R_i(C_{pq}) + u_i^{C_{pq}} S_i(C_{pq}) \Bigg] \end{aligned}$$

where $\zeta_{1,i}^{C_{pq}}$, $\zeta_{2,i}^{C_{pq}}$ and $\zeta_{3,i}^{C_{pq}}$ are the adjoint functions to be determined suitably. We obtain the following theorem

Theorem 4.1. *(Necessary Conditions) Given an optimal control ${u^{C_{pq}}}^*$ and solutions $S^*(C_{pq}), I^*(C_{pq})$ and $R^*(C_{pq})$, there exists $\zeta_{k,i}^{C_{pq}}, i = 0...N, k = 1,2,3$, the adjoint variables satisfying the following equations*

$$\begin{aligned}
\Delta\zeta_{1,i}^{C_{pq}} &= -\left[\zeta_{1,i+1}^{C_{pq}}\left(1-\sum_{C_{rs}\in\mathscr{V}'_{pq}} pot(i,C_{rs})-\gamma_{pq}(C_{pq})I_i(C_{pq})-\sum_{C_{rs}\in\mathscr{V}'_{pq}}\gamma_{pq}(C_{rs})I_i(C_{rs})-m-u_i^{C_{pq}}\right)\right. \\
&\left.\zeta_{2,i+1}^{C_{pq}}\left(\gamma_{pq}(C_{pq})I_i(C_{pq})+\sum_{C_{rs}\in\mathscr{V}'_{pq}}\gamma(C_{rs})I_i(C_{rs})\right)+\zeta_{3,i+1}^{C_{pq}}u_i^{C_{pq}}\right] \qquad (10)\\
\Delta\zeta_{2,i}^{C_{pq}} &= -\Big[A-\zeta_{1,i+1}^{C_{pq}}\gamma_{pq}(C_{pq})S_i(C_{pq}) \\
&+\zeta_{2,i+1}^{C_{pq}}\left(1-\sum_{C_{rs}\in\mathscr{V}'_{pq}} pot(i,C_{rs})+\gamma_{pq}(C_{pq})S_i(C_{pq})-(m+\rho+\lambda)\right)+\zeta_{3,i+1}^{C_{pq}}*\lambda\Big] \qquad (11)\\
\Delta\zeta_{3,i}^{C_{pq}} &= -\zeta_{3,i+1}^{C_{pq}}\left(1-\sum_{C_{rs}\in\mathscr{V}'_{pq}} pot(i,C_{rs})-m\right) \qquad (12)
\end{aligned}$$

where $\zeta_{1,N}^{C_{pq}}=0, \zeta_{2,N}^{C_{pq}}=A, \zeta_{3,N}^{C_{pq}}=0$, are the transversality conditions. In addition

$$\begin{aligned}
{u_i^{C_{pq}}}^* &= min\{max\{\frac{(\zeta_{1,i+1}^{C_{pq}}-\zeta_{3,i+1}^{C_{pq}})S_i(C_{pq})}{\tau}, u^{min}\}, u^{max}\}, \qquad (13)\\
&\quad i=0,...,N-1
\end{aligned}$$

Proof. Using Pontryagin's Maximum Principle [35] and setting $S^*(C_{pq})$, $I^*(C_{pq})$ and $R^*(C_{pq})$ and ${u^{C_{pq}}}^*$ we obtain the following adjoint equations:

$$\begin{aligned}
\Delta\zeta_{1,i}^{C_{pq}} &= -\frac{\partial H}{\partial S_i(C_{rs})} \\
&= -\left[\zeta_{1,i+1}^{C_{pq}}\left(1-\sum_{C_{rs}\in\mathscr{V}'_{pq}} pot(i,C_{rs})-\gamma_{pq}(C_{pq})I_i(C_{pq})-\sum_{C_{rs}\in\mathscr{V}'_{pq}}\gamma_{pq}(C_{rs})I_i(C_{rs})-m-u_i^{C_{pq}}\right)\right. \\
&\left.\zeta_{2,i+1}^{C_{pq}}\left(\gamma_{pq}(C_{pq})I_i(C_{pq})+\sum_{C_{rs}\in\mathscr{V}'_{pq}}\gamma_{pq}(C_{rs})I_i(C_{rs}\right)+\zeta_{3,i+1}^{C_{pq}}u_i^{C_{pq}}\right]
\end{aligned}$$

$$\begin{aligned}
\Delta\zeta_{2,i}^{C_{pq}} &= -\frac{\partial H}{\partial I_i(C_{rs})} \\
&= -\Big[A-\zeta_{1,i+1}^{C_{pq}}\gamma_{pq}(C_{pq})S_i(C_{pq}) \\
&\quad +\zeta_{2,i+1}^{C_{pq}}\left(1-\sum_{C_{rs}\in\mathscr{V}'_{pq}} pot(i,C_{rs})+\gamma_{pq}(C_{pq})S_i(C_{pq})-(m+\rho+\lambda)\right)+\zeta_{3,i+1}^{C_{pq}}*\lambda\Big] \\
\Delta\zeta_{3,i}^{C_{pq}} &= -\frac{\partial H}{\partial R_i(C_{rs})} \\
&= -\zeta_{3,i+1}^{C_{pq}}\left(1-\sum_{C_{rs}\in\mathscr{V}'_{pq}} pot(i,C_{rs})-m\right)
\end{aligned}$$

with transversality conditions

$$\zeta_{1,N}^{C_{pq}}=0,\zeta_{2,N}^{C_{pq}}=A,\zeta_{3,N}^{C_{pq}}=0$$

To obtain the optimality conditions we take the variation with respect to control ${u_i^{C_{pq}}}^*$ and set it equal to zero

$$\frac{\partial H}{\partial u_i^{C_{pq}}}=\tau u_i^{C_{pq}}-\zeta_{1,i+1}^{C_{pq}}S_i(C_{pq})+\zeta_{3,i+1}^{C_{pq}}S_i(C_{pq})=0.$$

Then we obtain the optimal control

$${u_i^{C_{pq}}}^*=\frac{(\zeta_{1,i+1}^{C_{pq}}-\zeta_{3,i+1}^{C_{pq}})S_i(C_{pq})}{\tau}.$$

By the bounds in $\mathscr{U}_{ad}$ of the control, it is easy to obtain ${u_i^{C_{pq}}}^*$ in the following form

$${u_i^{C_{pq}}}^*=\max\{\min\{\frac{(\zeta_{1,i+1}^{C_{pq}}-\zeta_{3,i+1}^{C_{pq}})S_i(C_{rs})}{\tau},u_{max}\},u_{min}\},\quad i=0,\ldots,N-1.$$

□

CONFLICT OF INTERESTS

The author(s) declare that there is no conflict of interests.

REFERENCES

[1] Wim Bernasco and Floor Luykx. Effects of attractiveness, opportunity and accessibility to burglars on residential burglary rates of urban neighborhoods. Criminology, 41(3)(2003), 981–1002.

[2] Jolita Sinkienė and Saulius Kromalcas. Concept, directions and practice of city attractiveness improvement. Public Policy and Admin., 31(1)(2010), 147–154.

[3] Hem Raj Joshi. Optimal control of an hiv immunology model. Opt. Control Appl. Methods, 23(4)(2002), 199–213.

[4] Omar Zakary, Mostafa Rachik, and Ilias Elmouki. On the impact of awareness programs in hiv/aids prevention: an sir model with optimal control. Int. J. Comput. Appl., 133(9)(2016), 1–6.

[5] Yinggao Zhou, Yiting Liang, and Jianhong Wu. An optimal strategy for hiv multitherapy. J. Comput. Appl. Math., 263(2014), 326–337.

[6] Collins Bekoe. The sir model and the 2014 ebola virus disease outbreak in guinea, liberia and sierra leone. Int. J. Appl. Sci., 6(2)(2015), 11-24.

[7] Sylvain Baize, Delphine Pannetier, Lisa Oestereich, Toni Rieger, Lamine Koivogui, N'Faly Magassouba, Barrè Soropogui, Mamadou Saliou Sow, Sakoba Keïta, Hilde De Clerck, et al. Emergence of zaire ebola virus disease in guinea. New Engl. J. Med., 371(15)(2014), 1418–1425.

[8] Shu Liao and Jim Wang. Stability analysis and application of a mathematical cholera model. Mathematical Biosciences and engineering, 8(3)(2011), 733–752.

[9] Jianjun Paul Tian and Jin Wang. Global stability for cholera epidemic models. Math. Biosci., 232(1)(2011), 31–41.

[10] Xueying Wang and Jin Wang. Analysis of cholera epidemics with bacterial growth and spatial movement. J. Biol. Dyn., 9(sup1)(2015), 233–261.

[11] Byul Nim Kim, Kyeongah Nah, Chaeshin Chu, Sang Uk Ryu, Yong Han Kang, and Yongkuk Kim. Optimal control strategy of plasmodium vivax malaria transmission in korea. Osong Public Health Res. Perspect., 3(3)(2012), 128–136.

[12] Olivia Prosper, Nick Ruktanonchai, and Maia Martcheva. Optimal vaccination and bednet maintenance for the control of malaria in a region with naturally acquired immunity. J. Theor. Biol., 353(2014), 142–156.

[13] FB Agusto. Optimal isolation control strategies and cost-effectiveness analysis of a two-strain avian influenza model. Biosystems, 113(3)(2013), 155–164.

[14] Julien Arino, Fred Brauer, Pauline Van Den Driessche, James Watmough, and Jianhong Wu. A model for influenza with vaccination and antiviral treatment. J. Theor. Biol., 253(1)(2008), 118–130.

[15] Linda JS Allen. Some discrete-time si, sir, and sis epidemic models. Math. Biosci., 124(1)(1994), 83–105.

[16] Kathryn Dabbs. Optimal control in discrete pest control models. University of Tennessee Honors Thesis Projects. 2010.

[17] Mustapha Lhous, Mostafa Rachik, and Abdelilah Larrache. Free optimal time control problem for a seir-epidemic model with immigration of infective. Int. J. Comput. Appl, 159(3)(2017), 1–5.

[18] Hem Raj Joshi, Suzanne Lenhart, Michael Y Li, and LIancheng Wang. Optimal control methods applied to disease models. Contemp. Math., 410(2006), 187–208.

[19] Omar Zakary, Mostafa Rachik, and Ilias Elmouki. On the analysis of a multi-regions discrete sir epidemic model: an optimal control approach. Int. J. Dyn. Control, 5(3)(2017), 917–930.

[20] Omar Zakary, Mostafa Rachik, and Ilias Elmouki. A new analysis of infection dynamics: multi-regions discrete epidemic model with an extended optimal control approach. Int. J. Dyn. Control, 5(4)(2017), 1010–1019.

[21] Omar Zakary, Mostafa Rachik, and Ilias Elmouki. A multi-regional epidemic model for controlling the spread of ebola: awareness, treatment, and travel-blocking optimal control approaches. Math. Methods Appl. Sci., 40(4)(2017), 1265–1279.

[22] Omar Zakary, Mostafa Rachik, and Ilias Elmouki. A new epidemic modeling approach: Multi-regions discrete-time model with travel-blocking vicinity optimal control strategy. Infect. Dis. Model., 2(3)(2017), 304–322.

[23] Omar Zakary, Mostafa Rachik, Ilias Elmouki, and Samih Lazaiz. A multi-regions discrete-time epidemic model with a travel-blocking vicinity optimal control approach on patches. Adv. Difference Equations, 2017(2017), 120.

[24] Haut Commissariat au Plan. Population légale. http://www.data.gov.ma/data/fr/dataset/population-legale, 2014.

[25] TAZI Ouadia, Abdelilah FAHDE, and Samira EL YOUNOUSSI. Impact de la pollution sur l'unique réseau hydrographique de casablanca, maroc. Science et changements planétaires/Sécheresse, 12(2)(2001), 129–34.

[26] Sonia Altizer, Rebecca Bartel, and Barbara A Han. Animal migration and infectious disease risk. Science, 331(6015)(2011), 296–302.

[27] HJ Koch and MJ Heuts. Regulation osmotique, cycle sexuel et migration de reproduction chez les epinoches. Arch. Int. Phys., 53(3-4)(1943), 253–266.

[28] Delphine Doctrinal, Dominique Bicout, Michel Gauthier-Clerc, Marc Artois, Alain Sandoz, and Philippe Sabatier. Rôle des oiseaux dans l'écologie de la fiévre du nil occidental: exemple du héron gardeboeuf en camargue. Environnement, Risques & Santé, 4(2)(2005), 101–108.

[29] A Tamisier, A Béchet, G Jarry, J-C Lefeuvre, and Y Le Maho. Effets du dérangement par la chasse sur les oiseaux d'eau: Revue de littérature. Revue d'écologie, 2003.

[30] Vincent H Resh and Ring T Cardé. Encyclopedia of insects. Academic press, 2009.

[31] Frédéric Gilli. Déplacements domicile-travail et organisation du bassin parisien. LEspace Geograph., 31(4)(2002), 289–305.

[32] Julien Talbot. Les déplacements domicile-travail: de plus en plus d'actifs travaillent loin de chez eux. 2001.

[33] Aurélien Delas. L'hôpital public, un nouvel acteur territorial entre aménagement sanitaire et rivalités stratégiques. Hérodote, 4(2011), 89–119.

[34] Olivier Badot and Jean-François Lemoine. Élargissement des principes de l'attractivité commerciale à ceux de l'attractivité touristique: le cas de la vallée village à marne-la-vallée. Manage. Avenir, 3(2015), 187–203.

[35] Lev Semenovich Pontryagin. Mathematical theory of optimal processes. Routledge, 2018.